BIOCHEMISTRY
including biophysical chemistry & molecular biology

Article

pubs.acs.org/biochemistry

Evidence for the Kinetic Partitioning of Polymerase Activity on G-Quadruplex DNA

Sarah Eddy,[†] Leena Maddukuri,[†] Amit Ketkar,[†] Maroof K. Zafar,[†] Erin E. Henninger,[‡] Zachary F. Pursell,[‡] and Robert L. Eoff*,[†]

[†]Department of Biochemistry and Molecular Biology, University of Arkansas for Medical Sciences, Little Rock, Arkansas 72205-7199, United States

[‡]Department of Biochemistry and Molecular Biology, Tulane University School of Medicine, 1430 Tulane Avenue, New Orleans, Louisiana 70112, United States

Supporting Information

ABSTRACT: We have investigated the action of the human DNA polymerase ε (hpol ε) and η (hpol η) catalytic cores on G-quadruplex (G4) DNA substrates derived from the promoter of the c-MYC proto-oncogene. The translesion enzyme hpol η exhibits a 6.2-fold preference for binding to G4 DNA over non-G4 DNA, while hpol ε binds both G4 and non-G4 substrates with nearly equal affinity. Kinetic analysis of single-nucleotide insertion by hpol η reveals that it is able to maintain >25% activity on G4 substrates compared to non-G4 DNA substrates, even when the primer template junction is positioned directly adjacent to G22 (the first tetrad-associated guanine in the c-MYC G4 motif). Surprisingly, hpol η fidelity increases ∼15-fold when copying G22. By way of comparison, hpol ε retains ∼4% activity and has a 33-fold decrease in fidelity when copying G22. The fidelity of hpol η is ∼100-fold greater than that of hpol ε when comparing the misinsertion frequencies of the two enzymes opposite a tetrad-associated guanine. The kinetic differences observed for the B- and Y-family pols on G4 DNA support a model in which a simple kinetic switch between replicative and TLS pols could help govern fork progress during G4 DNA replication.

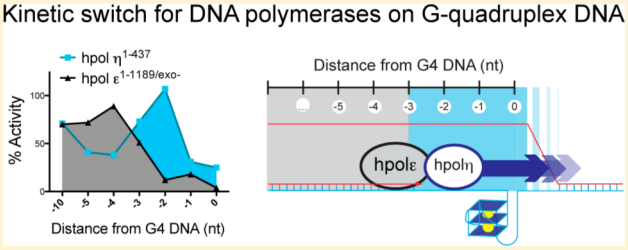

Many obstacles must be overcome to accurately replicate the genome. Exposure to reactive chemicals or radiation can produce a variety of damaged DNA structures that block replication and are etiological factors in many types of cancer.[1,2] The human genome encodes at least 17 different DNA polymerases (pols), including high-fidelity replicative pols and lower-fidelity translesion synthesis (TLS) pols. Nucleotide selection by high-fidelity replicative pols, such as the B-family member pol ε (hpol ε), is restricted by structural and kinetic parameters that impair catalysis on damaged templates.[3] TLS pols, on the other hand, are able to function in the replication of damaged templates because they possess structural attributes that allow them to accommodate bulky and/or distorted DNA lesions.[4] Foremost among the TLS enzymes are those of the Y-family, which in humans includes pols η, ι, κ, and Rev1. Mutations in the gene that encodes hpol η can cause the skin cancer-prone disease xeroderma pigmentosum variant.[5] Accordingly, the TLS activity of hpol η is found to be involved in the bypass of UV-induced cyclobutane pyrimidine dimers (CPDs).[6,7] Additional studies have implicated hpol η action in resistance to anticancer treatments, especially platinum-based drugs, as well as in the replication of common fragile sites (CFSs).[8,9] The structural properties that facilitate hpol η-catalyzed bypass of DNA lesions are multifaceted, but two features are central to the effective bypass of the aforementioned blocks to replication (i.e., CPDs, Pt-GG adducts, and CFSs): (i) hpol η can accommodate CPD and Pt-GG adducts in its large active site, and (ii) the hpol η DNA-binding cleft acts as a "molecular splint" that is able to maintain damaged/distorted template DNA in an undistorted form.[6] Additionally, it has been postulated that the back of the little finger domain serves as a "wedge" to mediate bypass of non-B-form DNA based on contacts between symmetry-related molecules in hpol η crystal structures.[6]

In addition to DNA adducts, blocks to replication arise from natural barriers, such as certain G-rich sequences that form G-quadruplex DNA (G4 DNA, also called QDNA or GQ).[10] G4 DNA sequences adopt secondary structures with unusually slow unfolding rates, and in cells, they appear to form maximally during S phase.[11,12] G4 motifs are positioned nonrandomly in functional regions of prokaryotic and eukaryotic genomes.[13] Several different G-quadruplexes have been studied in great structural and biophysical detail, including G4 structures derived from the *c-MYC* promoter.[14] The relevance of these sequences to human disease is illustrated by the enrichment of G4 DNA sites in the promoters of many oncogenes, at telomeres, at replication origins, and at chromosomal breakpoints in a variety of cancer types.[14−20]

Received: January 22, 2015
Revised: April 1, 2015
Published: April 23, 2015

DOI: 10.1021/acs.biochem.5b00060
Biochemistry 2015, 54, 3218−3230

Thus, defective maintenance of G4 DNA sequences contributes to genomic instability and is especially relevant to cancer.

Replication of G4 motifs requires proteins and enzymes with specific functions. It is well-known that Y-family pols are important for TLS past DNA adducts,[21,22] and it is becoming increasingly recognized that Y-family DNA pols are important for maintaining fork progress past non-B-form DNA structures, such as G4 DNA.[23−28] As early as 2006, studies in *Caenorhabditis elegans* revealed that Y-family pols η and κ are responsible for preventing deletions in G4 motifs in strains deficient in the FANCJ helicase.[28] Additional studies showed that human cells depleted of either pol η or κ exhibit increased levels of double-strand break formation and cell death following exposure to G4 DNA-binding ligands when extra genomic copies of the *c-MYC* G4 DNA sequence are present.[23] More recently, two reports have illustrated that the Y-family member Rev1 is required for maintaining fork progression past G4 DNA sites in avian cells.[26,27] One study used complementation assays in *rev1* deficient DT40 cells to implicate both the catalytic activity and the polymerase interacting region of Rev1 in the successful replication of G4 DNA.[27] A second study by the same groups revealed that Rev1 functions in coordination with FANCJ to maintain replication fork integrity during bypass of G4 DNA and that loss of Rev1 could be supplanted by either BLM or WRN RecQ helicases.[26] Thus, a model has been proposed recently for G4 DNA replication that involves the actions of either RecQ helicases or the TLS pol Rev1 functioning in coordination with FANCJ helicase.[26] Still, the precise function of Y-family pols (and proteins associated with their activity) during G4 DNA replication remains unclear, as the appropriate structure−function studies are lacking.

To elucidate the mechanistic basis for TLS pol action during replication of G4 DNA, we have investigated human pols from two different families: the catalytic cores of the B-family member hpol ε (amino acids 1−1189) and the Y-family member hpol η (amino acids 1−437). In an effort to systematically analyze the catalytic competence of each enzyme on G4 DNA, we performed DNA binding assays along with kinetic analysis of nucleotide insertion on both control non-G4 DNA substrates and DNA substrates possessing a G4-forming sequence derived from the *c-MYC* promoter. We find that, at the binding step, the TLS enzyme hpol η^{1-437} interacts preferentially with G4 DNA substrates, while hpol ε^{1-1189} binds non-G4 and G4 DNA substrates with equal affinity. The catalytic core of the leading strand enzyme, hpol ε^{1-1189}, exhibits inhibition of activity near G4 structures, whereas hpol η^{1-437} maintains relatively robust activity when copying tetrad-associated guanines. Finally, we observe a curious increase in the fidelity of hpol η^{1-437} on G4 DNA substrates relative to non-G4 control substrates, whereas the fidelity of exonuclease deficient (exo$^-$) hpol $\varepsilon^{1-1189/exo-}$ decreases sharply near G4 DNA. Our results show that a partitioning of pol activity can occur during replication of G-quadruplex structures based on DNA binding and kinetic parameters of nucleotidyl transfer alone (i.e., in the absence of accessory factors and/or protein−protein interactions). Taken together, our *in vitro* study is consistent with the idea that binding and catalytic properties of individual pols at sites of G4 DNA could help govern fork progress past these endogenous barriers to replication.

MATERIALS AND METHODS

Materials. All chemicals were molecular biology grade or better. 2′-Deoxynucleoside triphosphates (dNTPs) were obtained from Promega (Piscataway, NJ). All oligonucleotides used in this work were synthesized by Integrated DNA Technologies (Coralville, IA). All primers used in the polymerization assays were labeled with 5′-6-carboxyfluorescein (FAM). For DNA polymerization assays, seven primer−template DNA (p/t-DNA) substrates were prepared with one of two 42-mer template strands (i.e., seven non-G4 control p/t-DNA substrates and seven G4 p/t-DNA substrates) for a total of 14 substrates (Table 1).

DNA Substrate Preparation. Oligonucleotide stock solutions were prepared as described previously.[29] Briefly, oligonucleotides were resuspended in 50 mM HEPES (pH 7.5) buffer. The primer−template substrates were prepared in 50 mM HEPES (pH 7.5) buffer containing either KCl (100 mM)

Table 1. Sequences of DNA Substrates Used in This Study

Substrates used in DNA binding assays:

1. 11/28-mer non-G4 DNA
5′-ATCCTCCCCTA-3′
3′-TAGGAGGGGATGGGTCGTATCAGTGTAT-/FAM/-5′
2. 11/28-mer G4 DNA[a]
5′-ATCCTCCCCTA-3′
3′-TAGGAGGGGAT**GGGTGGGATGGGTGGGT**-/FAM/-5′

Substrates used in DNA pol activity assays:

1. 13/42-mer non-G4 DNA
5′-/FAM/-TTTGCCTCGAGCCAGC-3′
3′-CGGAGCTCGGTCGGCGTCTGCGTGGGTACCAGTTGTAGAGTG-5′
2. 18/42-mer non-G4 DNA
5′-/FAM/-TTTGCCTCGAGCCAGCCGCAG-3′
3′-CGGAGCTCGGTCGGCGTCTGCGTGGGTACCAGTTGTAGAGTG-5′
3. 19/42-mer non-G4 DNA
5′-/FAM/-TTTGCCTCGAGCCAGCCGCAGA-3′
3′-CGGAGCTCGGTCGGCGTCTGCGTGGGTACCAGTTGTAGAGTG-5′
4. 20/42-mer non-G4 DNA
5′-/FAM/-TTTGCCTCGAGCCAGCCGCAGAC-3′
3′-CGGAGCTCGGTCGGCGTCTGCGTGGGTACCAGTTGTAGAGTG-5′
5. 21/42-mer non-G4 DNA
5′-/FAM/-TTTGCCTCGAGCCAGCCGCAGACG-3′
3′-CGGAGCTCGGTCGGCGTCTGCGTGGGTACCAGTTGTAGAGTG-5′
6. 22/42-mer non-G4 DNA
5′-/FAM/-TTTGCCTCGAGCCAGCCGCAGACGC-3′
3′-CGGAGCTCGGTCGGCGTCTGCGTGGGTACCAGTTGTAGAGTG-5′
7. 23/42-mer non-G4 DNA
5′-/FAM/-TTTGCCTCGAGCCAGCCGCAGACGCA-3′
3′-CGGAGCTCGGTCGGCGTCTGCGTGGGTACCAGTTGTAGAGTG-5′
8. 13/42-mer G4 DNA
5′-/FAM/-TTTGCCTCGAGCCAGC-3′
3′-CGGAGCTCGGTCGGCGTCTGCGT**GGGTGGGATGGGTGGG**AGT-5′
9. 18/42-mer G4 DNA
5′-/FAM/-TTTGCCTCGAGCCAGCCGCAG-3′
3′-CGGAGCTCGGTCGGCGTCTGCGT**GGGTGGGATGGGTGGG**AGT-5′
10. 19/42-mer G4 DNA
5′-/FAM/-TTTGCCTCGAGCCAGCCGCAGA-3′
3′-CGGAGCTCGGTCGGCGTCTGCGT**GGGTGGGATGGGTGGG**AGT-5′
11. 20/42-mer G4 DNA
5′-/FAM/-TTTGCCTCGAGCCAGCCGCAGAC-3′
3′-CGGAGCTCGGTCGGCGTCTGCGT**GGGTGGGATGGGTGGG**AGT-5′
12. 21/42-mer G4 DNA
5′-/FAM/-TTTGCCTCGAGCCAGCCGCAGACG-3′
3′-CGGAGCTCGGTCGGCGTCTGCGT**GGGTGGGATGGGTGGG**AGT-5′
13. 22/42-mer G4 DNA
5′-/FAM/-TTTGCCTCGAGCCAGCCGCAGACGC-3′
3′-CGGAGCTCGGTCGGCGTCTGCGT**GGGTGGGATGGGTGGG**AGT-5′
14. 23/42-mer G4 DNA
5′-/FAM/-TTTGCCTCGAGCCAGCCGCAGACGCA-3′
3′-CGGAGCTCGGTCGGCGTCTGCGT**GGGTGGGATGGGTGGG**AGT-5′

[a]Tetrad-associated guanines are shown in bold with the G22 guanine underlined.

DOI: 10.1021/acs.biochem.5b00060
Biochemistry 2015, 54, 3218−3230

or NaCl (100 mM) by adding the primer and template strands (1:2 primer:template molar ratio), heating the sample to 95 °C for 5 min, and then slowly cooling it to room temperature.

Protein Expression and Purification. The core pol domain of hpol η (residues 1−437) was expressed in bacteria and purified as described previously.[30] The core pol domain of hpol ε (residues 1−1189) was expressed in bacteria and purified in a manner similar to what has been described previously.[31] Both wild-type and exonuclease deficient (exo$^-$) versions of hpol ε^{1-1189} were prepared. Site-directed mutagenesis was used to introduce Pol ε-exo$^-$ mutations D275A and E277A. Pol ε-pGEX4T3 expression vectors were cotransformed into Rosetta cells (EMD Millipore) with the TEV-pRK603 vector to allow for intracellular cleavage of the N-terminal GST tag by TEV protease. An aliquot of an overnight culture of Rosetta cells containing the hpol ε-N140 expression vector was added to 6 L of LB medium to a final A_{600} of 0.1. Cells were grown at 37 °C while being shaken at 220 rpm to an OD_{600} of 0.6, and then expression was induced by 4 μM isopropyl β-D-1-thiogalactopyranoside for 4 h at room temperature. Cells were harvested by centrifugation and resuspended in lysis buffer [150 mM Tris (pH 7.8) buffer containing 50 mM NaCl, 10 mM K_2SO_4, 0.25 mM EDTA, and protease inhibitor tablets (Roche) at 1.5 mL/g of cells]. A French press was used to lyse cells, and clarified lysates were purified with a HisTrapFF column (GE Healthcare). The column equilibration/wash solution consisted of 150 mM Tris (pH 7.8) buffer containing 200 mM NaCl, 20 mM K_2SO_4, and 2 mM dithiothreitol (DTT). Bound protein was washed with 25 column volumes (c.v.) of wash buffer, followed by 10 c.v. of wash buffer containing 75 mM imidazole, and then eluted in 150 mM imidazole. Protein was dialyzed overnight into size-exclusion chromatography (SEC) buffer, which consisted of 150 mM Tris (pH 7.8) buffer containing 200 mM NaCl, 20 mM K_2SO_4, and 2 mM DTT. The protein was then resolved by a Superdex 200 10/300 GL column (GE Healthcare). Purified samples were stored in SEC buffer supplemented with 10% (v/v) glycerol at −80 °C.

Measurement of DNA Binding Affinity by Fluorescence Polarization. Two DNA substrates were prepared for binding assays (Table 1). Substrates were prepared as described above. DNA binding affinity was measured by incubating DNA substrates (1 nM) with varying concentrations of enzyme (0−1 μM for hpol η^{1-437} and 0−0.4 μM for hpol ε^{1-1189}). Fluorescence polarization was measured in a Biotek Synergy4 plate reader using the appropriate filter sets (λ_{ex} = 485 ± 20 nm, and λ_{em} = 525 ± 20 nm). All titrations were performed at 25 °C in 50 mM HEPES (pH 7.5) buffer containing 10 mM KOAc, 10 mM KCl, 5 mM $MgCl_2$, 0.1 mM EDTA, 2 mM β-mercaptoethanol (β-ME), and 0.1 mg/mL bovine serum albumin (BSA). Polarization was determined using eq 1:

$$P = \frac{F_{\parallel} - F_{\perp}}{F_{\parallel} + F_{\perp}} \quad (1)$$

where $F_{\parallel}$ is the fluorescence intensity parallel to the excitation plane and $F_{\perp}$ the fluorescence intensity perpendicular to the excitation plane. Fluorescence polarization data were plotted as a function of enzyme concentration and then fit to the equation $P = P_0 + P_{max}\{D_t + E_t + K_{d,DNA} - [(D_t + E_t + K_{d,DNA})^2 - 4D_tE_t]^{1/2}\}/(2D_t)$, where P is the measured change in polarization (millipolarization units, mP), P_0 is the initial polarization value derived from the fit, P_{max} is the maximal change in polarization, D_t is the DNA concentration, E_t is the enzyme concentration, and $K_{d,DNA}$ is the equilibrium dissociation constant for binding of enzyme to DNA.

Pol Extension Assays. A FAM-labeled primer (18 nucleotides in length) was annealed to either a 42-nucleotide non-G4 control template oligonucleotide or a 42-nucleotide G4-forming sequence derived from the *c-MYC* promoter for use in pol extension assays (Table 1). DNA substrates (200 nM) were incubated at 37 °C with 5 nM hpol η^{1-437} or hpol ε^{1-1189}. Reactions were initiated by adding a dNTP·$MgCl_2$ solution (each dNTP at 0.25 mM and either 10 or 8 mM $MgCl_2$ for hpol η^{1-437} and hpol ε^{1-1189}, respectively) to the preincubated pol·DNA complex. All enzymatic reactions were conducted at 37 °C in 40 mM HEPES (pH 7.5) buffer containing 5 mM DTT, 100 μg/mL BSA, 5% (v/v) glycerol, and either 100 mM KCl or 100 mM NaCl. At time points of up to 6 h, 4 μL aliquots were quenched with 36 μL of a 95% (v/v) formamide/20 mM EDTA/0.1% (w/v) bromophenol blue solution and separated by electrophoresis on a 12% (w/v) polyacrylamide/7 M urea gel. The products were then visualized using a Typhoon imager (GE Healthcare Life Sciences) and quantified using ImageJ.[32]

Steady-State Kinetic Analysis of dNTP Insertion by Pols. Single-nucleotide insertion by both hpols η and ε was measured over a range of dNTP concentrations. Fourteen p/t-DNA substrates were used (Table 1; seven non-G4 p/t-DNA substrates and seven G4 p/t-DNA substrates) to assess the effect of varying the primer length on DNA pol activity. To obtain estimates for Michaelis−Menten kinetic parameters, non-G4 and G4 p/t-DNA substrates (200 nM) were preincubated with either hpol η^{1-437} (2 nM) or hpol $\varepsilon^{1-1189/exo-}$ (5 nM), and the reactions were initiated by addition of the appropriate dNTP (0−200 μM) and $MgCl_2$ (5 and 8 mM for hpol η^{1-437} and hpol $\varepsilon^{1-1189/exo-}$, respectively). All the enzymatic reactions were conducted at 37 °C in 40 mM HEPES (pH 7.5) buffer containing 100 mM KCl, 5 mM DTT, 0.1 mg/mL BSA, and 5% (v/v) glycerol. Experiments with hpol η^{1-437} proceeded for up to 30 min before 4 μL aliquots of the reaction were quenched with 36 μL of a 95% (v/v) formamide/20 mM EDTA/0.1% (w/v) bromophenol blue solution (Figure S1 of the Supporting Information). In experiments with hpol $\varepsilon^{1-1189/exo-}$, dNTP concentrations of >10 μM were quenched at 1.5 h, while dNTP concentrations of <10 μM were allowed to proceed for 3 h before being quenched (Figure S2 of the Supporting Information). Reaction products were separated by electrophoresis on a 12% (w/v) polyacrylamide/7 M urea gel except for reactions with substrates possessing the 13-mer primer, which were separated on a 16% (w/v) polyacrylamide/7 M urea gel. The products were then visualized using a Typhoon imager (GE Healthcare Life Sciences) and quantified using ImageJ.[32] Because hpol $\varepsilon^{1-1189/exo-}$ is highly processive, conditions for single-nucleotide insertion on the 23/42-mer substrate could not be obtained because the primer positions the enzyme across from three consecutive template guanines; therefore, the three product bands were quantified for reactions with G4 and non-G4 23/42-mer DNA to yield a value for total product as opposed to quantification of a single band for all other p/t-DNA substrates. The initial rate of product formation was plotted as a function of dNTP concentration and fit to the one-site hyperbolic equation in Prism (GraphPad, San Diego, CA). The turnover number (k_{cat}) and Michaelis constant ($K_{M,dNTP}$) are reported.

Analysis of Pol Misinsertion Frequency. The misinsertion frequency of both hpol η^{1-437} and hpol $\varepsilon^{1-1189/exo-}$

DOI: 10.1021/acs.biochem.5b00060
Biochemistry 2015, 54, 3218−3230

was measured over a range of dNTP concentrations for 21/42-mer, 22/42-mer, and 23/42-mer G4 and non-G4 DNA substrates. A pilot study was first conducted with both hpol η^{1-437} and hpol $\varepsilon^{1-1189/exo-}$ to determine the identity of the most favored misinsertion product (Figures S3 and S4 of the Supporting Information). Kinetic analysis of dNTP misinsertion was then performed with hpol η^{1-437} (2 nM) and hpol $\varepsilon^{1-1189/exo-}$ (5 nM) for the six DNA substrates (200 nM). Reactions were initiated by adding dNTP (0−1 mM for hpol η^{1-437} and 0−2.5 mM for hpol $\varepsilon^{1-1189/exo-}$) and $MgCl_2$ (5 mM for hpol η^{1-437} and 8 mM for hpol $\varepsilon^{1-1189/exo-}$). The reactions were quenched as described above. Misinsertion of dTMP was measured for hpol η^{1-437} on the 21/42-mer, 22/42-mer, and 23/42-mer G4 and non-G4 DNA substrates. For hpol $\varepsilon^{1-1189/exo-}$, misinsertion of dGMP opposite template dG was measured for 21/42-mer and 23/42-mer DNA substrates with both G4 and non-G4 sequences. Misinsertion of dCMP opposite template dT was measured for hpol $\varepsilon^{1-1189/exo-}$ with both G4 and non-G4 22/42-mer DNA substrates. Incorporation of dCMP opposite template dT by hpol $\varepsilon^{1-1189/exo-}$ resulted in multiple misinsertion product bands on 22/42-mer non-G4 DNA, as did misinsertion of dGMP on 23/42-mer DNA substrates. Therefore, total product was quantified for hpol $\varepsilon^{1-1189/exo-}$ misinsertion reactions on 22/42-mer and 23/42-mer DNA substrates. For experiments with hpol η^{1-437}, 4 μL aliquots were added to 36 μL of quench solution at time points of up to 3 h; 4 μL aliquots of hpol $\varepsilon^{1-1189/exo-}$ reactions were quenched at 8 h. Reaction products were separated, visualized, and analyzed as described in the previous section.

RESULTS

Comparison of Binding of hpol ε^{1-1189} and hpol η^{1-437} to *c-MYC* G4 DNA Substrates. We first analyzed the binding properties of recombinant hpol η^{1-437} and hpol ε^{1-1189} by titrating the enzyme into a solution of FAM-labeled p/t-DNA and measuring changes in fluorescence polarization for either non-G4 DNA or G4 DNA substrates (Figure 1). Two 11/28-mer DNA substrates (Table 1) were prepared in a solution containing K^+ (100 mM), and salt-dependent G-quadruplex formation for G4 substrates was assessed using circular dichroism (CD) and dimethyl sulfate (DMS) footprinting (data not shown). Fitting the fluorescence polarization data to a quadratic equation resulted in an estimate of the equilibrium dissociation constant for binding of pol to DNA ($K_{d,DNA}$). The Y-family member hpol η^{1-437} binds G4 DNA-containing substrates with an affinity approximately 6.2-fold higher than that for non-G4 substrates (Figure 1a). The measured $K_{d,DNA}$ values for hpol η^{1-437} binding were 87 ± 11 nM for the non-G4 control substrate and 14 ± 2 nM for the G4 DNA substrate. We then measured the affinity of the catalytic core of the eukaryotic leading strand pol, hpol ε^{1-1189}. The measured $K_{d,DNA}$ values for hpol ε^{1-1189} binding were 280 ± 39 nM for the non-G4 control substrate and 223 ± 42 nM for the G4 DNA substrate. These values are slightly higher than but comparable to the $K_{d,DNA}$ (79 nM) reported for the hpol ε^{1-1189} catalytic core recently using chemical quench assays.[33] However, the authors of the previous study performed the pol reactions at 20 °C, and they did not add any salt to the reaction buffers used to measure pol activity, which will undoubtedly alter the DNA binding properties of hpol ε. We observe a 1.3-fold difference in measured $K_{d,DNA}$ values for the two substrates used here (Figure 1b), which suggests that hpol ε^{1-1189} does not discriminate between G4 and non-G4 DNA at

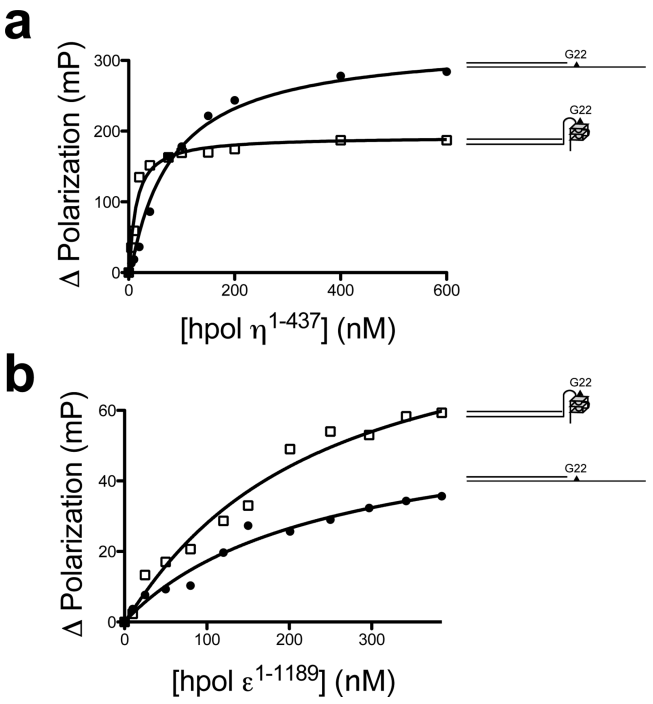

Figure 1. Y-Family member hpol η^{1-437} preferentially binds G4 DNA-containing substrates. (a) hpol η^{1-437} was titrated into a solution containing either G4 DNA (□) or non-G4 DNA (●) FAM-labeled 11/28-mer primer−template oligonucleotides (1 nM). Changes in fluorescence polarization were measured and the resulting data fit to a quadratic equation to yield the following equilibrium dissociation constants: G4 DNA, $K_{d,DNA}$ = 14 ± 2 nM; non-G4 DNA, $K_{d,DNA}$ = 87 ± 11 nM. The reported K_d values represent the mean ± sem (n = 3). (b) hpol ε^{1-1189} was titrated into a solution containing either G4 DNA (□) or non-G4 DNA (●) FAM-labeled 11/28-mer primer−template oligonucleotides (1 nM). Changes in fluorescence polarization were measured and the resulting data fit to a quadratic equation to yield the following equilibrium dissociation constants: primer−template G4 DNA, $K_{d,DNA}$ = 223 ± 42 nM; primer−template non-G4 DNA, $K_{d,DNA}$ = 280 ± 39 nM. The reported K_d values represent the mean ± sem (n = 2).

the binding step. Although these results were obtained with the hpol ε catalytic core, it is likely the same would hold true for the holoenzyme because a previous study reported that the small subunits of yeast pol ε had no impact on ssDNA binding capacity.[34] After comparison of the two enzymes, it would seem that hpol η has a stronger preference for binding G4 DNA substrates than the replicative enzyme.

Running Start Primer Extension Activities for hpol ε^{1-1189} and η^{1-437} on G4 DNA Substrates. Running start pol extension assays were conducted as an initial, qualitative assessment of differences in enzymatic activity toward G4 DNA substrates. Total extended product formed in each of the four reactions was quantified to calculate the percent activity of each pol on G4 DNA by dividing the amount of product in the G4 reaction by the amount of product in the control reaction. Contrasting the percent activity values allowed us to make a relative comparison of pol activity toward G4 DNA. The 18-mer primer used for these experiments positions the terminal 3′-OH group five nucleotides from the first tetrad guanine (G22) in the template strand (Figure 2a). Initially, we compared both G4 and non-G4 DNA substrates in reaction solutions containing 100 mM potassium. As expected, both enzymes pause in the presence of G4 DNA (Figure 2b).

DOI: 10.1021/acs.biochem.5b00060
Biochemistry 2015, 54, 3218−3230

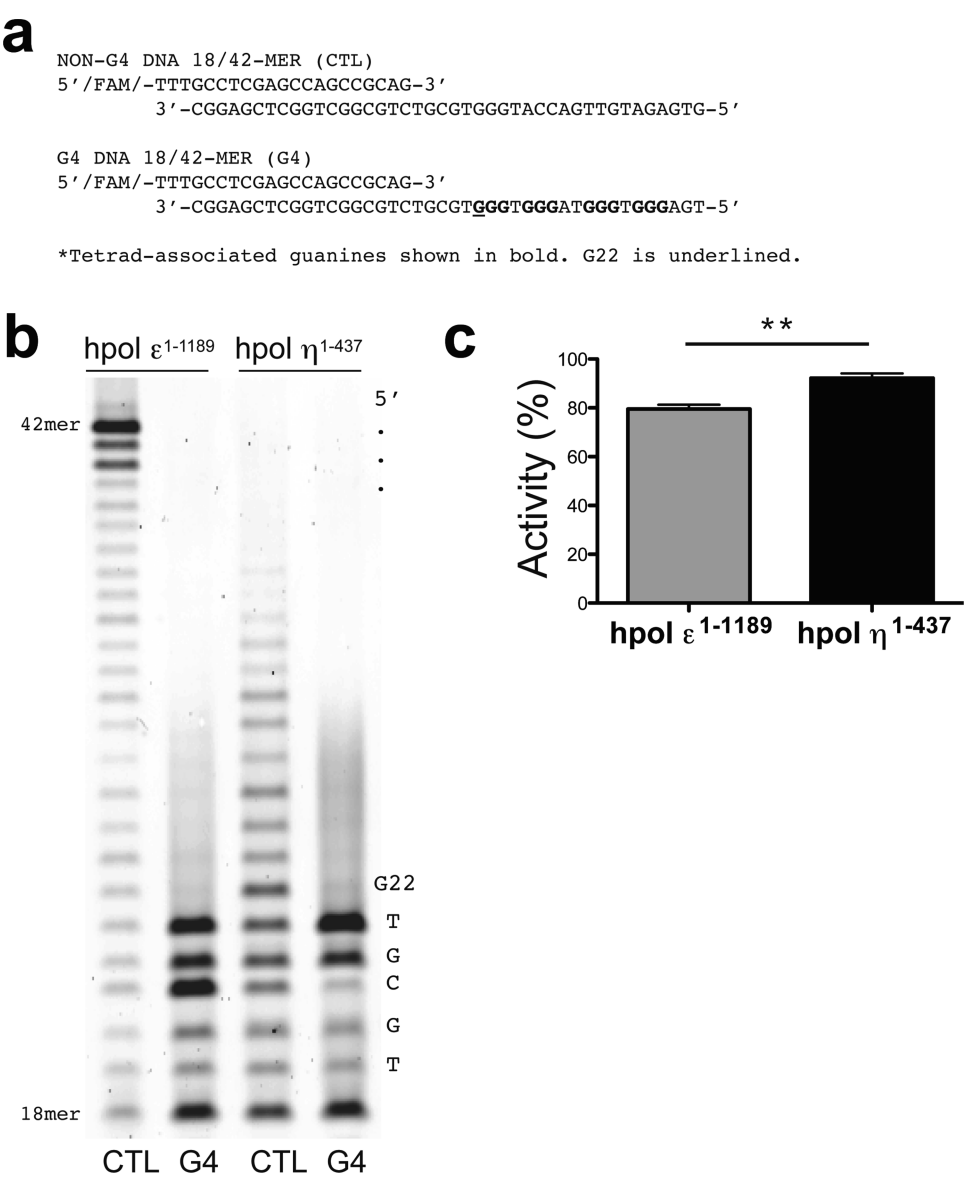

Figure 2. hpol η^{1-437} and hpol ε^{1-1189} extension activity on G4 DNA substrates. (a) Running start pol extension assays were performed with non-G4 DNA (CTL) and G4 DNA (G4) 18/42-mer p/t-DNA substrates. The tetrad-associated guanines in the G4 substrate are shown in bold, with the G22 position underlined. (b) Each enzyme (5 nM) was incubated with 18/42-mer p/t-DNA (200 nM), and pol extension was allowed to proceed in the presence of a mixture of all four dNTPs (250 μM) for 3 h at 37 °C. The pol extension products were separated by electrophoresis on a 12% (w/v) polyacryamide/7 M urea gel. The identities of the template bases just 3′ to the first tetrad guanine (G22) are noted to the side of the gel. (c) The total product formed in each of the pol extension assays was quantified. Dividing the total product formed for G4 DNA by the product formed in the CTL reaction and multiplying by 100 resulted in a percent activity on the G4 DNA value for both enzymes. The TLS pol, hpol η^{1-437}, retained 92.2 ± 1.9% activity on G4 substrates (n = 3). The replicative enzyme, hpol ε^{1-1189}, retained 79.5 ± 1.8% activity on G4 substrates (n = 3). The reported values represent the mean ± sem. A two-tailed unpaired t test comparing the values for the two enzymes resulted in P = 0.0084.

However, there are two important differences that are noticeable upon comparison of the gel results for the two enzymes. First, hpol ε^{1-1189} exhibits a strong pause two nucleotides from G22, whereas hpol η^{1-437} can synthesize DNA up to the first tetrad guanine without much pausing. The second feature of note in the running start experiment is the amount of primer converted to product by each enzyme. In the reaction with hpol ε^{1-1189}, there is clearly less primer extension occurring in the experiment with G4 DNA than in the non-G4 experiment, where essentially all of the primer is extended (Figure 2b; note the different intensities of the 18-mer substrate band on the gel for the two hpol ε^{1-1189} experiments). This is in contrast to the amount of primer extended by the Y-family member, hpol η^{1-437}, for which the difference in unutilized primer between the control and G4 DNA substrates is less dramatic (note the intensity of the 18-mer substrate band in the experiments with hpol η). These results indicate that the Y-family pol is able to perform catalysis on G4 substrates more effectively than the B-family member, hpol ε^{1-1189}. The replicative enzyme, hpol ε^{1-1189} exhibits 79.5 ± 1.8% activity on G4 substrates, while hpol η^{1-437} is 92.2 ± 1.9% active upon comparison of G4 substrates to non-G4 DNA (Figure 2c; P = 0.0084). We conclude that primer extension by the TLS enzyme hpol η^{1-437} is more efficient and proceeds closer to the G4 structure than the replicative enzyme, hpol ε^{1-1189}.

DOI: 10.1021/acs.biochem.5b00060
Biochemistry 2015, 54, 3218−3230

Because the Myc2345 14/23-mer G4 structure used in our assays is a highly stable quadruplex with a T_m of 75−85 °C (depending on the K^+ concentration),[35,36] we wanted to ascertain whether the two pols under investigation could copy a less stable version of the parallel-stranded *c-MYC* G4 structure. To test this idea, we prepared both the G4 and non-G4 DNA substrates in Na^+ (100 mM) and performed running start extension assays. While Na^+ can stabilize G-quadruplex structures, it is known to decrease the melting temperature of G4 DNA.[12] Indeed, experiments with hpol η^{1-437} reveal the less stable nature of a Na^+-bound G-quadruplex, as the Y-family member synthesizes across the G4 motif with a noticeably smaller reduction in the amount of fully extended product compared to that seen with hpol ε (Figure 3a). The replicative

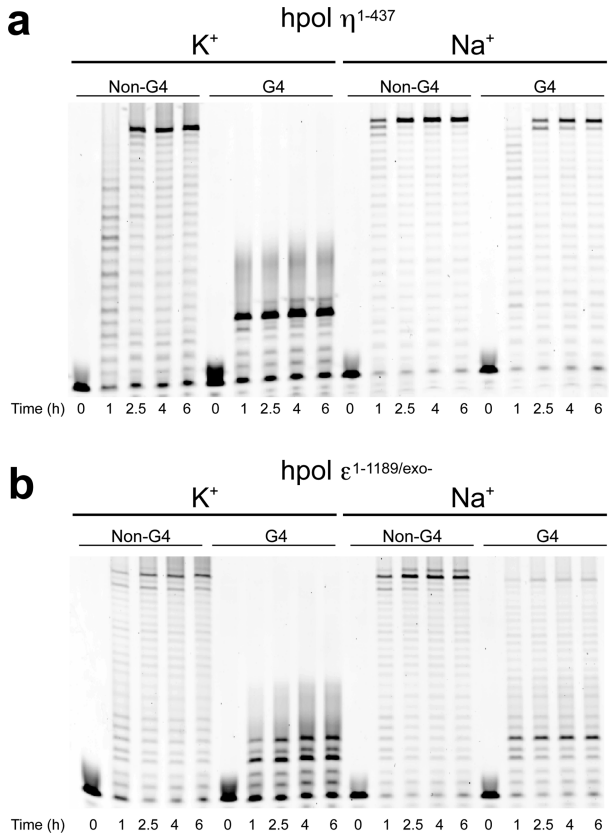

Figure 3. hpol η^{1-437} can efficiently copy G4 DNA stabilized by Na^+, but hpol ε^{1-1189} remains partially inhibited. (a) Running start pol extension time course experiments were performed with hpol η^{1-437} (5 nM) in the presence of either KCl or NaCl (100 mM) for both CTL and G4 18/42-mer p/t-DNA substrates (200 nM). DNA synthesis by hpol η^{1-437} proceeds essentially unperturbed when copying Na^+-stabilized G4 DNA. (b) Running start pol extension time course experiments were performed with hpol $\varepsilon^{1-1189/exo-}$ (5 nM) in the presence of either KCl or NaCl (100 mM) for both CTL and G4 18/42-mer p/t-DNA substrates (200 nM). DNA synthesis by hpol $\varepsilon^{1-1189/exo-}$ still shows a considerable amount of pausing on Na^+-stabilized G4 DNA substrates.

enzyme, hpol $\varepsilon^{1-1189/exo-}$, on the other hand, still exhibits a strong pause when attempting to copy the G4 motif, although the pause two nucleotides from G22 is diminished for Na^+-stabilized G4 DNA (Figure 3b). It becomes apparent from these results that the Na^+-stabilized G4 structure is not an impediment to hpol η activity, while hpol ε still has some difficulty in dealing with the less stable G-quadruplex.

Steady-State Kinetic Analysis of TLS Y-Family Member hpol η^{1-437} Activity on G4 DNA Substrates. To more closely examine the effect of G4 DNA on polymerization, we prepared a series of p/t-DNA substrates with varying primer lengths that positioned the 3′-OH from ten (13-mer primer) to zero (23-mer primer) nucleotides from G22, the first tetrad-associated guanine in the *c-MYC* G4 motif. A total of 14 p/t-DNA substrates were prepared (Table 1; seven non-G4 control substrates and seven G4 DNA substrates). We performed steady-state kinetic analysis of single-nucleotide insertion for the correct dNTP by hpol η^{1-437} on each of the 14 DNA substrates. The relative activity of hpol η^{1-437} on G4 DNA was calculated by measuring the specificity constant ($k_{cat}/K_{m,dNTP}$) on G4 DNA and dividing that value by the specificity constant of the enzyme on non-G4 DNA substrates. In this way, we were able to systematically evaluate how the catalytic efficiency of hpol η^{1-437} changes as the enzyme approaches the G4 structure.

When hpol η^{1-437} is positioned ten nucleotides from G22, its activity is essentially unperturbed (Table 2). Somewhat surprisingly, there is a drop in hpol η^{1-437} relative activity to ∼40% when the primer terminus is positioned five nucleotides from the G4 structure. However, hpol η^{1-437} is able to maintain

Table 2. Steady-State Kinetic Parameters for hpol η^{1-437} Catalysis on G4 DNA and Non-G4 DNA Substrates

	k_{cat} (min^{-1})	$K_{M,dNTP}$ (μM)	$k_{cat}/K_{M,dNTP}$ (min^{-1} μM^{-1})	relative activity[a]
13/42-mer: dCMP insertion opposite Template dG −10 Nucleotides from G22				
non-G4 DNA	10 ± 1	33 ± 3	0.30	–
G4 DNA	9.6 ± 0.2	44 ± 3	0.22	73%
18/42-mer: dAMP insertion opposite Template dT −5 Nucleotides from G22				
non-G4 DNA	9.2 ± 0.7	14 ± 3	0.66	–
G4 DNA	12 ± 1	44 ± 6	0.27	41%
19/42-mer: dCMP insertion opposite Template dG −4 Nucleotides from G22				
non-G4 DNA	26 ± 1	11 ± 2	2.4	–
G4 DNA	23 ± 2	25 ± 4	0.92	38%
20/42-mer: dGMP insertion opposite Template dC −3 Nucleotides from G22				
non-G4 DNA	11 ± 1	20 ± 2	0.55	–
G4 DNA	9.2 ± 0.2	23 ± 1	0.40	73%
21/42-mer: dCMP insertion opposite Template dG −2 Nucleotides from G22				
non-G4 DNA	18 ± 1	27 ± 5	0.67	–
G4 DNA	15 ± 1	21 ± 3	0.71	107%
22/42-mer: dAMP insertion opposite Template dT −1 Nucleotide from G22				
non-G4 DNA	7.7 ± 0.3	26 ± 3	0.30	–
G4 DNA	5.1 ± 0.2	55 ± 3	0.09	31%
23/42-mer: dCMP insertion opposite G22				
non-G4 DNA	20 ± 1	5.4 ± 0.9	3.7	–
G4 DNA	11 ± 1	12 ± 2	0.92	25%

[a]Relative activity was calculated as $[(k_{cat}/K_{m,dNTP})_{G4\ DNA}/(k_{cat}/K_{m,dNTP})_{non\text{-}G4\ DNA}] \times 100$. For determination of all kinetic values, initial estimates for the rate of product formation were followed by titration experiments (10−12 concentrations of dNTP; $n = 1$). Graphs of the initial rate of product formation vs dNTP concentration were plotted using nonlinear regression analysis (one-site hyperbolic fit) in GraphPad Prism. The standard error of the fit is reported for each kinetic parameter.

DOI: 10.1021/acs.biochem.5b00060
Biochemistry 2015, 54, 3218−3230

fairly robust activity on G4 substrates as the primer terminus is moved closer to the G-quadruplex structure. Interestingly, hpol η^{1-437} activity on G4 substrates increases back to levels comparable to that of the control substrate when the primer is positioned two to three nucleotides from the G-quadruplex (Table 2; see Results for the 20/42- and 21/42-mer substrates). These kinetic results correspond well to the qualitative running start primer extension assays (Figure 2b), in which there is very little pausing by hpol η^{1-437} as the primer is extended to 20 and 21 nucleotides, indicative of efficient pol activity. The catalytic efficiency of hpol η^{1-437} decreases to 31% when the primer is positioned one nucleotide from G22 (Table 2; see Results for the 22/42-mer DNA substrate). The relative activity of hpol η^{1-437} is ~25% when the enzyme inserts dCMP opposite the tetrad guanine G22 (Table 2; see Results for the 23/42-mer substrates). The general trend that underlies the decrease in hpol η^{1-437} catalytic efficiency on G4 substrates is an increase in the Michaelis constant ($K_{m,dNTP}$), although there is a 43% reduction in the k_{cat} for the insertion of dCMP opposite G22 (Table 2; see Results for the 23/42-mer substrates). For most of the substrates, the turnover number (k_{cat}) describing hpol η^{1-437}-catalyzed nucleotidyl transfer is essentially unchanged by the presence of G4 DNA compared to changes in the measured $K_{m,dNTP}$ values. Overall, the single-nucleotide results for hpol η^{1-437} are indicative of an enzyme that is reasonably tolerant of a very stable intramolecular G-quadruplex in the template strand, even when the G4 DNA structure is in the proximity of the pol active site.

Measurement of hpol η^{1-437} Misinsertion Frequency on G4 DNA Substrates. We next wanted to examine the effect of G4 DNA on the misinsertion frequency (f_{ins}) of hpol η^{1-437}. We focused our efforts on the three substrates that position the primer terminus two, one, or zero nucleotides from G22 (i.e., 21/42-mer, 22/42-mer, and 23/42-mer G4 and non-G4DNA, for a total of six DNA substrates). We determined the nucleotide that was most likely to be misinserted by performing a time course experiment measuring hpol η^{1-437}-catalyzed insertion of each of the incorrect dNTPs on the six DNA substrates used in the misinsertion experiments. In all cases, we found that hpol η^{1-437} preferred to misinsert dTMP. Steady-state kinetic analysis of dTMP misinsertion by hpol η^{1-437} was performed, and the misinsertion frequency on each substrate was estimated (Table 3). On the three non-G4 DNA substrates, hpol η^{1-437} makes a mistake roughly once every 13−300 catalytic events. The range of hpol η^{1-437} accuracy was found to be one mistake every 30−4800 catalytic events for the three G4 DNA substrates. Directly comparing the misinsertion frequency for each substrate pair, we find that the fidelity of DNA synthesis by hpol η^{1-437} is increased slightly (~8-fold) when the primer is positioned two nucleotides from the G4 motif (Table 3; compare f_{ins} for the 21/42-mer DNA substrates). There is an approximate 5-fold decrease in fidelity when hpol η^{1-437} is placed one nucleotide from the G4 motif (Table 3; compare f_{ins} for the 22/42-mer DNA substrates). Perhaps the most interesting change in fidelity was observed with the 23/42-mer substrate, for which hpol η^{1-437} fidelity is increased ~15-fold when it attempts to copy the tetrad guanine G22 (Table 3; compare f_{ins} for the 23/42-mer substrates). We conclude from these experiments that the fidelity of hpol η is impacted by the presence of G4 DNA, with misinsertion of dTMP across from the G22 tetrad guanine being so strongly inhibited by the G-quadruplex that the fidelity of hpol η is increased 15-fold.

Table 3. Steady-State Kinetic Parameters for hpol η^{1-437} Misinsertion on G4 DNA and Non-G4 DNA Substrates

	k_{cat} (min^{-1})	$K_{M,dNTP}$ (μM)	$k_{cat}/K_{M,dNTP}$ (min^{-1} μM^{-1})	f_{ins} [a]
21/42-mer: dTMP insertion opposite Template dG (−2 nucleotides from G22)				
non-G4 DNA	2.6 ± 0.3	53 ± 22	0.049	0.073
G4 DNA	1.3 ± 0.2	190 ± 80	0.0068	0.0096
22/42-mer: dTMP insertion opposite Template dT (−1 nucleotide from G22)				
non-G4 DNA	1.4 ± 0.1	730 ± 140	0.0019	0.0063
G4 DNA	1.4 ± 0.1	510 ± 110	0.0027	0.030
23/42-mer: dTMP insertion opposite Template dG (0 nucleotides from G22)				
non-G4 DNA	5.6 ± 0.8	450 ± 140	0.012	0.0032
G4 DNA	0.039 ± 0.003	200 ± 50	0.00019	0.00021

[a]The misinsertion frequency (f_{ins}) was calculated as $(k_{cat}/K_{M,incorrect\ dNTP})/(k_{cat}/K_{M,correct\ dNTP})$.

Steady-State Kinetic Analysis of Replicative B-Family Member hpol $\varepsilon^{1-1189/exo-}$ Activity on G4 DNA Substrates. So that we might gain some perspective on how the changes in hpol η^{1-437} catalytic efficiency and fidelity compared to those of other pols, we then went on to investigate how the replicative enzyme, hpol ε, was affected by G-quadruplexes. Exonuclease deficient hpol $\varepsilon^{1-1189/exo-}$ was used to measure single-nucleotide insertion kinetics. The same set of 14 p/t-DNA substrates was used to determine the relative activity of hpol $\varepsilon^{1-1189/exo-}$ on G4 DNA. The absolute values of the steady-state kinetic parameters obtained with hpol $\varepsilon^{1-1189/exo-}$ are different from those reported in a previous study,[31] resulting in a lower specificity constant for the DNA substrates tested here (Table 4). This is likely due to the higher salt concentrations required to investigate G-quadruplexes, as a previous report showed that 100 mM KCl or NaCl strongly inhibits the pol ε holoenzyme.[37] Recent pre-steady-state experiments have reported k_{pol} values of ~250−300 s^{-1} with yeast and human pol ε, in line with the values reported for other B-family pols.[33,38] However, the reaction buffer used in the pre-steady-state experiments with pol ε did not have any salt in them. Thus, the absolute values of the pre-steady-state kinetic constants reported might not represent what occurs at more physiological salt concentrations, such as the concentrations we have employed in our steady-state assays. The k_{cat} values reported here are approximately 5−10-fold lower than those calculated for hpol $\varepsilon^{1-1189/exo-}$ previously under the no salt reaction conditions.[31,33] However, the misinsertion frequencies measured by us (Table 5) are very similar to steady-state values reported previously under conditions of no salt,[31] which is a good indicator that the mechanism of nucleotide selection by hpol $\varepsilon^{1-1189/exo-}$ remains intact.

Steady-state kinetic analysis of hpol $\varepsilon^{1-1189/exo-}$-catalyzed correct nucleotide insertion was consistent with the running start extension assays in that the relative efficiency of catalysis by hpol $\varepsilon^{1-1189/exo-}$ drops substantially when the primer is positioned two nucleotides from G22 (Table 4). The drop in efficiency for hpol $\varepsilon^{1-1189/exo-}$ is driven by both an increase in the $K_{m,dNTP}$ and a decrease in the k_{cat}. The changes in both the k_{cat} and $K_{m,dNTP}$ values are also observed with the 22/42-mer and 23/42-mer substrates, with hpol $\varepsilon^{1-1189/exo-}$ activity dropping to <4% when the enzyme attempts to copy G22 in an accurate fashion. In short, hpol $\varepsilon^{1-1189/exo-}$ maintains good activity until the primer is positioned two to three nucleotides

DOI: 10.1021/acs.biochem.5b00060
Biochemistry 2015, 54, 3218−3230

Table 4. Steady-State Kinetic Parameters for hpol $\varepsilon^{1-1189/exo-}$ Catalysis on G4 DNA and Non-G4 DNA Substrates

	k_{cat} (min^{-1})	$K_{M,dNTP}$ (μM)	$k_{cat}/K_{M,dNTP}$ (min^{-1} μM^{-1})	relative activity[a]
13/42-mer: dCMP insertion opposite Template dG −10 Nucleotides from G22				
non-G4 DNA	0.31 ± 0.01	8.9 ± 2.1	0.035	–
G4 DNA	0.22 ± 0.01	8.6 ± 1.3	0.025	71%
18/42-mer: dAMP insertion opposite Template dT −5 Nucleotides from G22				
non-G4 DNA	0.42 ± 0.01	3.3 ± 0.6	0.13	–
G4 DNA	0.23 ± 0.01	2.5 ± 0.6	0.09	72%
19/42-mer: dCMP insertion opposite Template dG −4 Nucleotides from G22				
non-G4 DNA	0.27 ± 0.01	2.3 ± 0.6	0.12	–
G4 DNA	0.21 ± 0.01	2.0 ± 0.4	0.11	89%
20/42-mer: dGMP insertion opposite Template dC −3 Nucleotides from G22				
non-G4 DNA	0.42 ± 0.02	2.0 ± 0.5	0.21	–
G4 DNA	0.16 ± 0.01	1.5 ± 0.5	0.11	51%
21/42-mer: dCMP insertion opposite Template dG −2 Nucleotides from G22				
non-G4 DNA	0.33 ± 0.06	8.0 ± 1.5	0.041	–
G4 DNA	0.098 ± 0.004	19 ± 4	0.005	12%
22/42-mer: dAMP insertion opposite Template dT −1 Nucleotide from G22				
non-G4 DNA	0.25 ± 0.01	4.4 ± 0.1	0.057	–
G4 DNA	0.12 ± 0.01	12 ± 2	0.010	18%
23/42-mer: dCMP insertion opposite G22				
non-G4 DNA	0.44 ± 0.03	3.1 ± 1.5	0.14	–
G4 DNA	0.29 ± 0.08	52 ± 33	0.0056	4%

[a]Relative activity was calculated as described in footnote [a] of Table 2.

Table 5. Steady-State Kinetic Parameters for hpol $\varepsilon^{1-1189/exo-}$ Misinsertion on G4 DNA and Non-G4 DNA Substrates

	k_{cat} (min^{-1})	$K_{M,dNTP}$ (μM)	$k_{cat}/K_{M,dNTP}$ (min^{-1} μM^{-1})	f_{ins}[a]
21/42-mer: dGMP insertion opposite Template dG (−2 nucleotides from G22)				
non-G4 DNA	0.065 ± 0.005	280 ± 40	0.00023	0.0056
G4 DNA	0.019 ± 0.001	380 ± 90	0.00005	0.010
22/42-mer: dCMP insertion opposite Template dT (−1 nucleotide from G22)				
non-G4 DNA	0.046 ± 0.005	390 ± 150	0.00012	0.0021
G4 DNA	0.017 ± 0.001	220 ± 70	0.00008	0.0080
23/42-mer: dGMP insertion opposite Template dG (0 nucleotides from G22)				
non-G4 DNA	0.052 ± 0.004	600 ± 130	0.00009	0.00063
G4 DNA	0.015 ± 0.005	120 ± 35	0.00012	0.021

[a]The misinsertion frequency (f_{ins}) was calculated as described in footnote [a] of Table 3.

from G22, at which point the relative efficiency of the reaction decreases substantially.

Measurement of hpol $\varepsilon^{1-1189/exo-}$ Misinsertion Frequency on G4 DNA Substrates. Finally, we determined the effect of G4 DNA on the fidelity of hpol $\varepsilon^{1-1189/exo-}$ by measuring the steady-state misinsertion frequencies on the 21/42-mer, 22/42-mer, and 23/42-mer DNA substrates. We assessed the preference for misinsertion by hpol $\varepsilon^{1-1189/exo-}$ and found that hpol $\varepsilon^{1-1189/exo-}$ preferred to misinsert dGMP on the 21/42-mer and 23/42-mer substrates, while favoring misinsertion of dCMP on the 22/42-mer DNA. Comparing the misinsertion frequencies for non-G4 and G4 DNA substrates reveals that the fidelity of nucleotide selection by hpol $\varepsilon^{1-1189/exo-}$ is decreased when a G4 structure is present in the template strand (Table 5). The decrease in hpol $\varepsilon^{1-1189/exo-}$ fidelity occurs for all three G4 substrates tested, but it is most pronounced when the enzyme attempts to copy G22 (Table 5; see Results for 23/42-mer DNA). The accuracy of nucleotidyl transfer by hpol $\varepsilon^{1-1189/exo-}$ is decreased >30-fold on the 23/42-mer G4 DNA substrate. In fact, nucleotidyl transfer by hpol $\varepsilon^{1-1189/exo-}$ is ∼2 orders of magnitude more error-prone than hpol η^{1-437} on the 23/42-mer G4 DNA substrate (Tables 3 and 5; compare the value of f_{ins} for each enzyme with the 23/42-mer G4 DNA substrate). On the basis of the change in fidelity for the two enzymes tested here, it would seem that hpol η can copy G4 motifs in a manner more accurate and efficient than that of the catalytic core of the replicative enzyme, hpol ε.

DISCUSSION

Although originally thought to be an *in vitro* curiosity,[39] landmark studies have elucidated the structural diversity of G-quadruplexes,[18,20,35,36,40−43] and experimental strategies have shown that G4 DNA forms *in vivo* with a wide range of biological ramifications.[13,17,27,44−49] Recent studies have visualized G4 DNA in human cells and found that they are formed maximally during S phase when the double helix is converted to single-stranded intermediates.[11,50] Additionally, analysis of >2700 cancer samples revealed that G4 motifs are enriched near chromosomal breakpoints and act as "mutagenic factors" in a variety of tumors;[17] however, the proteins and enzymes required for successful G4 DNA replication are only now being elucidated, and many catalytic features relevant to DNA synthesis at G4 motifs remain unclear. The visualization of nontelomeric G4 structures during S phase and the ability of some intramolecular G-quadruplexes to fold on the millisecond time scale suggest the possibility that DNA pols might encounter fully or partially folded G4 DNA during replication.[11,51] Certain helicases and single-stranded DNA-binding proteins are critical for maintenance of G4 motifs, and a number of these proteins and enzymes are capable of unwinding G-quadruplexes *in vitro*.[26,48,52−55] What is less clear is why certain DNA pols appear to be required for replication of G4 DNA. We set out to determine if the biochemical properties of recombinant B- and Y-family DNA pols could help explain results obtained in genetic and cell culture-based experiments implicating a role for translesion enzymes in the maintenance of G-quadruplexes.[23,28] The binding and catalytic properties of the Y-family enzyme hpol η^{1-437} were compared to those of the B-family enzyme, hpol ε^{1-1189}, in an effort to improve our understanding of mechanisms of pol action during G4 DNA replication. We also compared the results reported here to those we reported previously for hRev1 using identical DNA substrates.[29]

Our biochemical results reveal important differences for B- and Y-family pols. First, we find that hpol η^{1-437} binds to G4 substrates with a 6.2-fold preference over non-G4 DNA. We do not observe a similar change in binding affinity for the replicative enzyme, hpol ε^{1-1189}. The increased binding affinity observed for hpol η^{1-437} with G4 DNA is not without precedent. We have shown previously that the catalytic core of another Y-family pol, hRev1$^{330-833}$, binds G4 DNA substrates with an affinity 15-fold greater than that for non-G4 DNA.[29] The increased binding affinity for TLS pols could certainly aid

DOI: 10.1021/acs.biochem.5b00060
Biochemistry 2015, 54, 3218−3230

in the localization of these specialized enzymes to G4 structures during replication fork stalling. However, preferred binding does not necessarily translate into robust catalytic properties on G4 DNA. For example, while hRev1 showed a considerable preference for binding to G4 substrates, the relative activity of nucleotide insertion by hRev1 opposite G22 was quite low (~2%) when compared to that measured for hpol η in the study presented here (25%). The relative activity of hRev1 was considerably better (~70%) when the enzyme was positioned four nucleotides from G22 (i.e., catalyzing insertion of dCMP opposite template dG on the 19/42-mer substrate). We were initially surprised by the lack of robust catalysis from hRev1 when copying the tetrad guanine G22 given its purported role in avian G4 replication. However, these results may not be so perplexing when one considers the fact that Rev1 is thought to function as a central scaffold for recruiting TLS pols to sites of replication stress through interactions in its C-terminus. Previous experiments from the Sale group implied that if Rev1 cannot recruit the other TLS pols then DNA synthesis across the G4 motif is impaired.[27] The low activity for hRev1 in catalyzing nucleotidyl transfer across from tetrad guanines could mean that DNA synthesis across the G4 motif is mainly performed by hpol η (or hpol κ), which was suggested previously by others and is consistent with both the kinetic results reported here and the defects in G4 replication reported in DT40 cells expressing a Rev1 C-terminal truncation mutant that cannot bind pol η or κ.[27] A model emphasizing a role for pol η (and/or pol κ) in performing DNA synthesis past G4 DNA is also in line with the deletion of G4 motifs observed in experiments with *C. elegans* mutants lacking FANCJ and either pol η or pol κ.[28] However, it is likely that Rev1 does copy some portion of the G4 motif in the template strand with the assistance of a helicase, such as FANCJ, because DT40 mutant cell lines expressing a catalytically inactive version of Rev1 exhibit a defect in G4 maintenance that is roughly half as strong as Rev1-null or Rev1 C-terminal deletion mutant cell lines.[26,27]

In addition to performing DNA binding studies, we systematically investigated the effect of G4 DNA on the single-nucleotide insertion kinetics of hpol η^{1-437} and hpol $\varepsilon^{1-1189/exo-}$ by varying the length of the primer on templates containing G4 DNA. Neither pol can completely bypass G4 DNA stabilized by K^+ (i.e., both enzymes pause on G4 substrates), but we do observe clear differences in the catalytic efficiencies of the two enzymes when the primer position is varied (Figure 4a). In agreement with the idea that replicative pols efficiently copy nonstructured DNA, hpol $\varepsilon^{1-1189/exo-}$ activity is higher than hpol η^{1-437} activity when the primer terminus is positioned four to five nucleotides from the G4 structure. However, hpol η^{1-437} activity increases dramatically when the 3′-OH group is placed two to three nucleotides from the first tetrad guanine (G22) and remains relatively robust even when copying G22, consistent with a role for this enzyme in performing DNA synthesis near G4 DNA structures. The most striking change in pol activity was obtained when we studied the kinetics of misinsertion by the two enzymes. Pol ε has the highest fidelity among yeast and human pols and, importantly, copies homonucleotide repeats, such as those found in G4 DNA substrates, more accurately than pol δ.[31,56] However, we find that the fidelity of hpol $\varepsilon^{1-1189/exo-}$ drops considerably on G4 substrates, especially when copying G22 (Table 5 and Figure 4b). Most surprisingly, hpol η^{1-437} fidelity increases 15-fold when the enzyme attempts to copy G22 (Table 3 and Figure 4b). These results are consistent with the

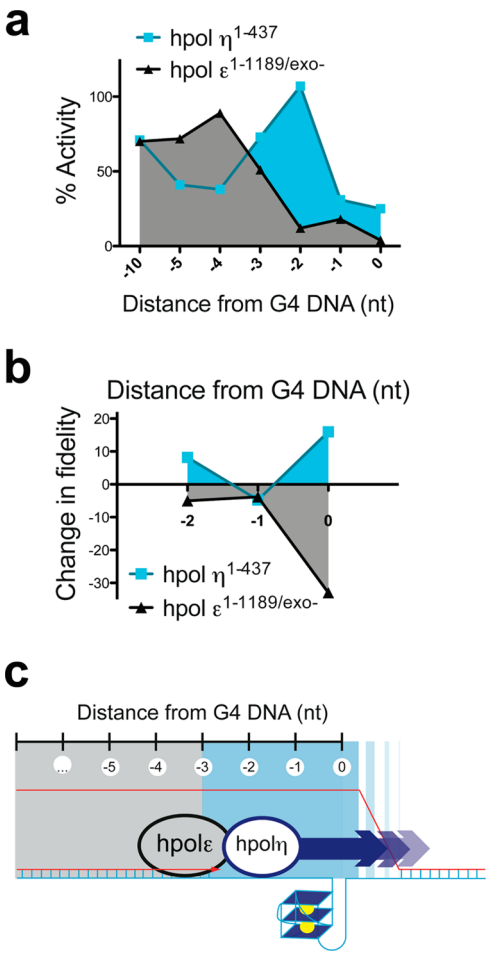

Figure 4. A simple kinetic switch between pols may promote more accurate and efficient replication of G4 DNA. (a) Relative activity of hpol η^{1-437} and hpol $\varepsilon^{1-1189/exo-}$ on G4 DNA plotted as a function of the distance from the primer terminus to the first tetrad guanine (G22). (b) Change in fidelity on G4 DNA substrates relative to control non-G4 for p/t-DNA substrates positioning the primer terminus two, one, and zero nucleotides from the first tetrad guanine (G22). (c) Cartoon illustration depicting the idea that DNA binding and kinetic properties of nucleotidyl transfer could partition hpol η and hpol ε activity during encounters with G4 DNA and that this division of labor may occur two to three nucleotides from G-quadruplex structures.

idea that changes in binding and catalysis for pols η and ε can partition the action of each enzyme on G4 DNA substrates (Figure 4c). While the catalytic activity of hpol η^{1-437} on G4 substrates is more efficient than that of either hpol ε^{1-1189} or hRev1$^{330-833}$ when the enzymes are positioned within three nucleotides of the G4 structure, it is by no means unaffected by the presence of G4 DNA. Rather, the degree to which catalysis by hpol η^{1-437} is perturbed implies that the enzyme could help maintain forward progress at sites where intramolecular G-quadruplexes have refolded in the path of the replisome but that it probably cannot perform this function alone.

The TLS enzyme hpol η is probably best known for its role in copying CPD lesions.[7,57,58] Binding of pol η to CPD-containing substrates is enhanced when a single 3′-adenosine is paired opposite the 3′-T in the dimer but destabilized once two adenosines are paired opposite the lesion,[59] which supports the increase in processivity that has been observed for pol η synthesis near CPD lesions.[7] The steady-state specificity

DOI: 10.1021/acs.biochem.5b00060
Biochemistry 2015, 54, 3218−3230

constants describing hpol η-catalyzed insertion opposite each damaged thymine in the T-T dimer are essentially unchanged, consistent with the idea that hpol η copies UV-induced T-T dimers very efficiently.[60] Moreover, the fidelity of hpol η is unaffected by the presence of the CPD lesion,[60] which is important for replication of CPDs. Another adduct that hpol η is thought to help bypass *in vivo* is the main intrastrand cross-linked product of cisplatin reactions with adjacent guanines (Pt-GG).[8,9,61] Kinetic analysis has revealed that hpol η copies the 3′-dG and 5′-dG sites within a Pt-GG adduct with catalytic efficiencies of 82 and 35%, respectively, relative to unmodified DNA.[62] However, the accuracy of nucleotide selection at the second insertion step (opposite the 5′-dG of the Pt-GG adduct) appears to be decreased on the basis of robust misinsertion of dAMP.[62] By way of comparison, G4 DNA is a greater impediment to efficient DNA synthesis by hpol η than either CPDs or Pt-GG adducts, but unlike bypass of the aforementioned adducts, the fidelity of nucleotide selection by hpol η is increased when inserting nucleotides opposite G22. The increased accuracy of hpol η on the 23/42-mer G4 substrate is primarily due to a large (~140-fold) decrease in the k_{cat} for misinsertion of dTMP opposite G22 (Table 3). If we extrapolate the kinetic results with hpol η into a cellular context, the G-quadruplex structure might be thought to be protecting the genome from increased levels of error-prone DNA synthesis by inhibiting TLS pol-catalyzed misinsertion. Loss of TLS pol action at these sites would be predicted to induce mutagenic replication, based on our results with hpol ε.

DNA pol strand-displacement activity has been reported on many occasions for short B-form dsDNA duplexes and is even the basis of a fluorescence-based screen for pol inhibitors.[63,64] However, it is unclear if DNA pols can promote unfolding of G4 DNA in the template strand by exerting a force on the nucleic acid structure as DNA synthesis is occurring. We have observed hRev1-dependent disruption of *c-MYC* G4 DNA in the absence of DNA synthesis that appears to be related to the ssDNA binding properties of that Y-family member.[25] For most pols, it seems unlikely that disruption of K^+-stabilized G4 structures with high melting temperatures, such as the *c-MYC* motif used here, would accompany DNA synthesis, but as one might expect, the degree of pol inhibition appears to change in manner that is dependent on the stability of the structure. The biophysical properties of G-quadruplexes are complex when one considers the sheer number of different topological arrangements, loop lengths, and folding dynamics associated with these structures.[12] One trend that seems to be shared by most (if not all) quadruplexes studied to date is the fact that K^+-bound G4 structures are more difficult to unfold than Na^+-bound G4 DNA. Substituting Na^+ for K^+ can decrease the T_m of telomeric G4 DNA by ~5−15 °C and result in ~1−4 kcal/mol decreases in $\Delta G_{(310)}$ values.[12] Unfolding of Na^+-stabilized telomeric G4 DNA, which is not as stable as the *c-MYC* G4 structure used in our assays, occurs when forces of <10 pN are applied.[65] The T7 DNA pol has been shown using single-molecule approaches to exert a force of ~30 pN during translocation.[66] Therefore, it may be possible for DNA pols to promote the unfolding of low-stability K^+-stabilized G4 structures or Na^+-stabilized G4 DNA, and it is reasonable to propose that both hpol ε and hpol η can act to varying degrees on Na^+-stabilized G4 structures in the template strand. On the basis of our results, it would appear that hpol η does indeed cause quadruplexes to unfold completely because we observe full-length primer extension on Na^+-stabilized G4 substrates (Figure 3a). Conversely, the high-fidelity enzyme hpol $\varepsilon^{1-1189/exo-}$ still exhibits a noticeable pause when it encounters the Na^+-stabilized G4 structure (Figure 3b), perhaps because of unfavorable interactions between the G4 structure and the domains comprising the ε active site.

A recent study with yeast and human pol δ reported that some pausing within telomeric TTAGGG repeat sequences occurred even under conditions where G-quadruplex formation is suppressed.[67] Extension assays with yeast and human pol δ showed that pausing is stronger when G-quadruplex formation is promoted,[67] although there does appear to be a non-G4-related factor that contributes to pol δ stuttering past homonucleotide repeats. Interestingly, both yeast and human pol δ show fairly strong pauses two nucleotides from the first run of telomeric tetrad guanines,[67] which is similar to what is observed with hpol ε (Figure 2). Direct comparisons to our results with hpol ε^{1-1189} are hampered by differing template sequences, as well as the fact that an equimolar ratio of pol δ to DNA was used to test for pol activity on telomeric G4 DNA. However, the fact that DNA synthesis by both hpol ε and hpol δ appears to be perturbed at a similar location on two different G4 template sequences is intriguing.

The structural basis for preferential interactions between Y-family pols and G4 DNA has yet to be defined. Crystal structures of hpol η provide some insight into how Y-family pols might accommodate G4 DNA in a manner that is distinct from those of other types of pols. The structure of hpol η reveals that two template bases are housed in the large active site for both undamaged and damaged DNA templates.[6,62] Additionally, template guanines in the hpol η active site have been observed in multiple conformations.[62] The accommodation of diverse template conformations is a hallmark of Y-family pol structure and function, and this property could promote productive interactions between hpol η and G4 DNA by allowing the enzyme to accept partially folded G4 structures. Furthermore, hpol η has been proposed to act as a "molecular splint" that maintains DNA in a B-form conformation even when adducts, such as CPD lesions, are present.[6] It is conceivable that contacts with multiple tetrad guanines near the hpol η active site could help prevent refolding of an intramolecular G-quadruplex. An additional point of contact between hpol η and G-quadruplex structures may involve a DNA-interacting surface that has been observed in the symmetry-related molecules of hpol η and was proposed to serve as a "wedge to separate non-B-form" DNA.[6] This secondary DNA-binding interface has both electrostatic (Arg^{81} and Arg^{84}) and base stacking (Trp^{339}) interactions between hpol η residues on the backside of the little finger and the symmetry-related DNA that are apparent in the crystal structures. These contacts may contribute to the preferential binding to G4 DNA by hpol η observed in our study, but experiments to test such a notion have yet to be reported. It is unclear how B-family pols might accommodate a fully or partially folded G4 structure. The crystal structure of yeast pol ε reveals that the enzyme does not make direct contact with any ssDNA template residues beyond the +1 position (i.e., the nucleotide in the template strand that is just 5′ of the nascent base pair).[68] The template residue in the +1 position must undergo a dramatic rotation as it moves into the yeast pol ε active site, a mechanistic feature that is conserved between B-family pols.[69,70] The inaccessibility of G4-associated guanines likely interferes with this base flipping event and is consistent

DOI: 10.1021/acs.biochem.5b00060
Biochemistry 2015, 54, 3218−3230

with our results showing a strong pause for hpol ε two nucleotides short of the first tetrad.

While DNA pols obviously function as part of the multisubunit replisome, our study is the first to provide evidence of a model in which kinetic partitioning of pol activity could govern fork progress during G4 DNA replication, providing further insight into why hpol η deficient cells have defects in the maintenance of sequences predicted to form G-quadruplexes.[23,28] Experiments to decipher the exact role for different Y-family pols at G4 sites in cells, as well as individual steps within the hpol η and hpol ε catalytic cycle that are modulated by G4 DNA, are ongoing. Regarding our results with hpol ε, it is important to note that our experiments were conducted with the catalytic core. It is possible that the hpol ε holoenzyme could display catalytic properties on G4 substrates that are different from the core because depletion of the two smallest subunits contributes to increased spontaneous mutagenesis in yeast.[71] The 3′−5′ exonuclease activity of hpol ε might also affect the fidelity of the enzyme. Thus, it will be interesting to assess the affect of G4 DNA on the proofreading action of hpol ε. Finally, it is worth noting that G4 structures appear to be oxidized more readily than non-G4 sequences because the oxidation potential of G4 guanines is expected to be lower than that of guanines in dsDNA.[72,73] The potential role for Y-family pol activity in the replication of damaged G4 DNA is an active area of investigation that could provide important insights into the mechanism(s) of TLS across from these non-B-form structures. In summary, the results reported here provide direct evidence of a simple kinetic switch between pols during G4 DNA replication, a mechanism that could prevent fork stalling at these sites in cells.

■ ASSOCIATED CONTENT

Supporting Information

Figures S1−S4 detail some of the steady-state kinetic experiments with the two polymerases. The Supporting Information is available free of charge on the ACS Publications website at DOI: 10.1021/acs.biochem.5b00060.

■ AUTHOR INFORMATION

Corresponding Author

*Department of Biochemistry and Molecular Biology, University of Arkansas Medical Sciences, Little Rock, AR 72205. E-mail: rleoff@uams.edu. Telephone: (501) 686-8343. Fax: (501) 686-8169.

Funding

This work was supported in part by the National Institutes of Health (Grants GM084460 and CA183895 to R.L.E. and Grants ES016780 and RR020152 to Z.F.P.) with additional support from the University of Arkansas for Medical Sciences Translational Research Institute (CTSA Grant UL1TR000039). Funding for open access charge provided by the University of Arkansas for Medical Sciences, College of Medicine.

Notes

The authors declare no competing financial interest.

■ ABBREVIATIONS

G4, G-quadruplex; dNTPs, deoxyribonucleotide triphosphates; DTT, dithiothreitol; EDTA, ethylenediaminetetraacetic acid; pol, (DNA) polymerase; FAM, 6-carboxyfluorescein; sem, standard error of the mean; TLS, translesion DNA synthesis.

■ REFERENCES

(1) Friedberg, E. C., Walker, G. C., Siede, W., Wood, R. D., Shultz, R. A., and Ellenberger, T. (2006) *DNA Repair and Mutagenesis*, 2nd ed., American Society for Microbiology Press, Washington, DC.

(2) Geacintov, N., and Broyde, S. (2010) *The Chemical Biology of DNA Damage*, Wiley-VCH, Weinheim, Germany.

(3) McCulloch, S. D., Kokoska, R. J., Chilkova, O., Welch, C. M., Johansson, E., Burgers, P. M., and Kunkel, T. A. (2004) Enzymatic switching for efficient and accurate translesion DNA replication. *Nucleic Acids Res. 32*, 4665−4675.

(4) Yang, W., and Woodgate, R. (2007) What a difference a decade makes: Insights into translesion DNA synthesis. *Proc. Natl. Acad. Sci. U.S.A. 104*, 15591−15598.

(5) Masutani, C., Kusumoto, R., Yamada, A., Dohmae, N., Yokoi, M., Yuasa, M., Araki, M., Iwai, S., Takio, K., and Hanaoka, F. (1999) The XPV (xeroderma pigmentosum variant) gene encodes human DNA polymerase η. *Nature 399*, 700−704.

(6) Biertümpfel, C., Zhao, Y., Kondo, Y., Ramon-Maiques, S., Gregory, M., Lee, J. Y., Masutani, C., Lehmann, A. R., Hanaoka, F., and Yang, W. (2010) Structure and mechanism of human DNA polymerase η. *Nature 465*, 1044−1048.

(7) McCulloch, S. D., Kokoska, R. J., Masutani, C., Iwai, S., Hanaoka, F., and Kunkel, T. A. (2004) Preferential cis-syn thymine dimer bypass by DNA polymerase η occurs with biased fidelity. *Nature 428*, 97−100.

(8) Albertella, M. R., Green, C. M., Lehmann, A. R., and O'Connor, M. J. (2005) A role for polymerase η in the cellular tolerance to cisplatin-induced damage. *Cancer Res. 65*, 9799−9806.

(9) Sokol, A. M., Cruet-Hennequart, S., Pasero, P., and Carty, M. P. (2013) DNA polymerase η modulates replication fork progression and DNA damage responses in platinum-treated human cells. *Sci. Rep. 3*, 3277.

(10) Murat, P., and Balasubramanian, S. (2014) Existence and consequences of G-quadruplex structures in DNA. *Curr. Opin. Genet. Dev. 25*, 22−29.

(11) Biffi, G., Tannahill, D., McCafferty, J., and Balasubramanian, S. (2013) Quantitative visualization of DNA G-quadruplex structures in human cells. *Nat. Chem. 5*, 182−186.

(12) Lane, A. N., Chaires, J. B., Gray, R. D., and Trent, J. O. (2008) Stability and kinetics of G-quadruplex structures. *Nucleic Acids Res. 36*, 5482−5515.

(13) Capra, J. A., Paeschke, K., Singh, M., and Zakian, V. A. (2010) G-Quadruplex DNA sequences are evolutionarily conserved and associated with distinct genomic features in *Saccharomyces cerevisiae*. *PLoS Comput. Biol. 6*, e1000861.

(14) Qin, Y., and Hurley, L. H. (2008) Structures, folding patterns, and functions of intramolecular DNA G-quadruplexes found in eukaryotic promoter regions. *Biochimie 90*, 1149−1171.

(15) Besnard, E., Babled, A., Lapasset, L., Milhavet, O., Parrinello, H., Dantec, C., Marin, J. M., and Lemaitre, J. M. (2012) Unraveling cell type-specific and reprogrammable human replication origin signatures associated with G-quadruplex consensus motifs. *Nat. Struct. Mol. Biol. 19*, 837−844.

(16) Cayrou, C., Coulombe, P., Puy, A., Rialle, S., Kaplan, N., Segal, E., and Mechali, M. (2012) New insights into replication origin characteristics in metazoans. *Cell Cycle 11*, 658−667.

(17) De, S., and Michor, F. (2011) DNA secondary structures and epigenetic determinants of cancer genome evolution. *Nat. Struct. Mol. Biol. 18*, 950−955.

(18) Henderson, E., Hardin, C. C., Walk, S. K., Tinoco, I., Jr., and Blackburn, E. H. (1987) Telomeric DNA oligonucleotides form novel intramolecular structures containing guanine-guanine base pairs. *Cell 51*, 899−908.

(19) Sundquist, W. I., and Klug, A. (1989) Telomeric DNA dimerizes by formation of guanine tetrads between hairpin loops. *Nature 342*, 825−829.

(20) Zahler, A. M., Williamson, J. R., Cech, T. R., and Prescott, D. M. (1991) Inhibition of telomerase by G-quartet DNA structures. *Nature 350*, 718−720.

DOI: 10.1021/acs.biochem.5b00060
Biochemistry 2015, 54, 3218−3230

(21) Friedberg, E. C., Wagner, R., and Radman, M. (2002) Specialized DNA polymerases, cellular survival, and the genesis of mutations. *Science 296*, 1627−1630.
(22) Woodgate, R. (1999) A plethora of lesion-replicating DNA polymerases. *Genes Dev. 13*, 2191−2195.
(23) Bétous, R., Rey, L., Wang, G., Pillaire, M. J., Puget, N., Selves, J., Biard, D. S., Shin-ya, K., Vasquez, K. M., Cazaux, C., and Hoffmann, J. S. (2009) Role of TLS DNA polymerases η and κ in processing naturally occurring structured DNA in human cells. *Mol. Carcinog. 48*, 369−378.
(24) Boyer, A. S., Grgurevic, S., Cazaux, C., and Hoffmann, J. S. (2013) The human specialized DNA polymerases and non-B DNA: Vital relationships to preserve genome integrity. *J. Mol. Biol. 425*, 4767−4781.
(25) Eddy, S., Ketkar, A., Zafar, M. K., Maddukuri, L., Choi, J. Y., and Eoff, R. L. (2014) Human Rev1 polymerase disrupts G-quadruplex DNA. *Nucleic Acids Res. 42*, 3272−3285.
(26) Sarkies, P., Murat, P., Phillips, L. G., Patel, K. J., Balasubramanian, S., and Sale, J. E. (2011) FANCJ coordinates two pathways that maintain epigenetic stability at G-quadruplex DNA. *Nucleic Acids Res. 40*, 1485−1498.
(27) Sarkies, P., Reams, C., Simpson, L. J., and Sale, J. E. (2011) Epigenetic instability due to defective replication of structured DNA. *Mol. Cell 40*, 703−713.
(28) Youds, J. L., O'Neil, N. J., and Rose, A. M. (2006) Homologous recombination is required for genome stability in the absence of DOG-1 in *Caenorhabditis elegans*. *Genetics 173*, 697−708.
(29) Eddy, S., Ketkar, A., Zafar, M. K., Maddukuri, L., Choi, J. Y., and Eoff, R. L. (2013) Human Rev1 polymerase disrupts G-quadruplex DNA. *Nucleic Acids Res. 42*, 3272−3285.
(30) Maddukuri, L., Ketkar, A., Eddy, S., Zafar, M. K., Griffin, W. C., and Eoff, R. L. (2012) Enhancement of human DNA polymerase η activity and fidelity is dependent upon a bipartite interaction with the Werner's syndrome protein. *J. Biol. Chem. 287*, 42312−42323.
(31) Korona, D. A., Lecompte, K. G., and Pursell, Z. F. (2010) The high fidelity and unique error signature of human DNA polymerase ϵ. *Nucleic Acids Res. 39*, 1763−1773.
(32) Schneider, C. A., Rasband, W. S., and Eliceiri, K. W. (2012) NIH Image to ImageJ: 25 years of image analysis. *Nat. Methods 9*, 671−675.
(33) Zahurancik, W. J., Klein, S. J., and Suo, Z. (2013) Kinetic mechanism of DNA polymerization catalyzed by human DNA polymerase ε. *Biochemistry 52*, 7041−7049.
(34) Tsubota, T., Tajima, R., Ode, K., Kubota, H., Fukuhara, N., Kawabata, T., Maki, S., and Maki, H. (2006) Double-stranded DNA binding, an unusual property of DNA polymerase ε, promotes epigenetic silencing in *Saccharomyces cerevisiae*. *J. Biol. Chem. 281*, 32898−32908.
(35) Ambrus, A., Chen, D., Dai, J., Jones, R. A., and Yang, D. (2005) Solution structure of the biologically relevant G-quadruplex element in the human c-MYC promoter. Implications for G-quadruplex stabilization. *Biochemistry 44*, 2048−2058.
(36) Mathad, R. I., Hatzakis, E., Dai, J., and Yang, D. (2011) c-MYC promoter G-quadruplex formed at the 5′-end of NHE III1 element: Insights into biological relevance and parallel-stranded G-quadruplex stability. *Nucleic Acids Res. 39*, 9023−9033.
(37) Chui, G., and Linn, S. (1995) Further characterization of HeLa DNA polymerase ε. *J. Biol. Chem. 270*, 7799−7808.
(38) Ganai, R. A., Osterman, P., and Johansson, E. (2015) Yeast DNA polymerase ε catalytic core and holoenzyme have comparable catalytic rates. *J. Biol. Chem. 290*, 3825−3835.
(39) Gellert, M., Lipsett, M. N., and Davies, D. R. (1962) Helix formation by guanylic acid. *Proc. Natl. Acad. Sci. U.S.A. 48*, 2013−2018.
(40) Hatzakis, E., Okamoto, K., and Yang, D. (2010) Thermodynamic stability and folding kinetics of the major G-quadruplex and its loop isomers formed in the nuclease hypersensitive element in the human c-Myc promoter: Effect of loops and flanking segments on the stability of parallel-stranded intramolecular G-quadruplexes. *Biochemistry 49*, 9152−9160.
(41) Phan, A. T., Kuryavyi, V., Burge, S., Neidle, S., and Patel, D. J. (2007) Structure of an unprecedented G-quadruplex scaffold in the human c-kit promoter. *J. Am. Chem. Soc. 129*, 4386−4392.
(42) Phan, A. T., Modi, Y. S., and Patel, D. J. (2004) Propeller-type parallel-stranded G-quadruplexes in the human c-myc promoter. *J. Am. Chem. Soc. 126*, 8710−8716.
(43) Sundquist, W. I., and Klug, A. (1989) Telomeric DNA dimerizes by formation of guanine tetrads between hairpin loops. *Nature 342*, 825−829.
(44) Azvolinsky, A., Dunaway, S., Torres, J. Z., Bessler, J. B., and Zakian, V. A. (2006) The *S. cerevisiae* Rrm3p DNA helicase moves with the replication fork and affects replication of all yeast chromosomes. *Genes Dev. 20*, 3104−3116.
(45) Huppert, J. L., and Balasubramanian, S. (2005) Prevalence of quadruplexes in the human genome. *Nucleic Acids Res. 33*, 2908−2916.
(46) Maizels, N. (2006) Dynamic roles for G4 DNA in the biology of eukaryotic cells. *Nat. Struct. Mol. Biol. 13*, 1055−1059.
(47) Müller, S., Kumari, S., Rodriguez, R., and Balasubramanian, S. (2010) Small-molecule-mediated G-quadruplex isolation from human cells. *Nat. Chem. 2*, 1095−1098.
(48) Paeschke, K., Capra, J. A., and Zakian, V. A. (2011) DNA replication through G-quadruplex motifs is promoted by the *Saccharomyces cerevisiae* Pif1 DNA helicase. *Cell 145*, 678−691.
(49) Schaffitzel, C., Berger, I., Postberg, J., Hanes, J., Lipps, H. J., and Pluckthun, A. (2001) *In vitro* generated antibodies specific for telomeric guanine-quadruplex DNA react with *Stylonychia lemnae* macronuclei. *Proc. Natl. Acad. Sci. U.S.A. 98*, 8572−8577.
(50) Lam, E. Y., Beraldi, D., Tannahill, D., and Balasubramanian, S. (2013) G-Quadruplex structures are stable and detectable in human genomic DNA. *Nat. Commun. 4*, 1796.
(51) Zhang, A. Y., and Balasubramanian, S. (2012) The kinetics and folding pathways of intramolecular G-quadruplex nucleic acids. *J. Am. Chem. Soc. 134*, 19297−19308.
(52) Li, J. L., Harrison, R. J., Reszka, A. P., Brosh, R. M., Jr., Bohr, V. A., Neidle, S., and Hickson, I. D. (2001) Inhibition of the Bloom's and Werner's syndrome helicases by G-quadruplex interacting ligands. *Biochemistry 40*, 15194−15202.
(53) Paeschke, K., Bochman, M. L., Garcia, P. D., Cejka, P., Friedman, K. L., Kowalczykowski, S. C., and Zakian, V. A. (2013) Pif1 family helicases suppress genome instability at G-quadruplex motifs. *Nature 497*, 458−462.
(54) Salas, T. R., Petruseva, I., Lavrik, O., Bourdoncle, A., Mergny, J. L., Favre, A., and Saintome, C. (2006) Human replication protein A unfolds telomeric G-quadruplexes. *Nucleic Acids Res. 34*, 4857−4865.
(55) Wu, Y., Shin-ya, K., and Brosh, R. M., Jr. (2008) FANCJ helicase defective in Fanconia anemia and breast cancer unwinds G-quadruplex DNA to defend genomic stability. *Mol. Cell. Biol. 28*, 4116−4128.
(56) Fortune, J. M., Pavlov, Y. I., Welch, C. M., Johansson, E., Burgers, P. M., and Kunkel, T. A. (2005) *Saccharomyces cerevisiae* DNA polymerase δ: High fidelity for base substitutions but lower fidelity for single- and multi-base deletions. *J. Biol. Chem. 280*, 29980−29987.
(57) Johnson, R. E., Prakash, S., and Prakash, L. (1999) Efficient bypass of a thymine-thymine dimer by yeast DNA polymerase, Pol η. *Science 283*, 1001−1004.
(58) Yoon, J. H., Prakash, L., and Prakash, S. (2009) Highly error-free role of DNA polymerase η in the replicative bypass of UV-induced pyrimidine dimers in mouse and human cells. *Proc. Natl. Acad. Sci. U.S.A. 106*, 18219−18224.
(59) Kusumoto, R., Masutani, C., Shimmyo, S., Iwai, S., and Hanoaka, F. (2004) DNA binding properties of human DNA polymerase η: Implications for fidelity and polymerase switching of translesion synthesis. *Genes Cells 9*, 1139−1150.
(60) Johnson, R. E., Washington, M. T., Prakash, S., and Prakash, L. (2000) Fidelity of human DNA polymerase η. *J. Biol. Chem. 275*, 7447−7450.
(61) Moraes, M. C., de Andrade, A. Q., Carvalho, H., Guecheva, T., Agnoletto, M. H., Henriques, J. A., Sarasin, A., Stary, A., Saffi, J., and Menck, C. F. (2012) Both XPA and DNA polymerase η are necessary

DOI: 10.1021/acs.biochem.5b00060
Biochemistry 2015, 54, 3218−3230

for the repair of doxorubicin-induced DNA lesions. *Cancer Lett. 314*, 108−118.
(62) Zhao, Y., Biertümpfel, C., Gregory, M. T., Hua, Y.-J., Hanoaka, F., and Yang, W. (2012) Structural basis of human DNA polymerase *η*-mediated chemoresistance to cisplatin. *Proc. Natl. Acad. Sci. U.S.A. 109*, 7269−7274.
(63) Dorjsuren, D., Wilson, D. M., III, Beard, W. A., McDonald, J. P., Austin, C. P., Woodgate, R., Wilson, S. H., and Simeonov, A. (2009) A real-time fluorescence method for enzymatic characterization of specialized human DNA polymerases. *Nucleic Acids Res. 37*, e128.
(64) Manosas, M., Spiering, M. M., Ding, F., Bensimon, D., Allemand, J.-F., Benkovic, S. J., and Croquette, V. (2012) Mechanism of strand displacement synthesis by DNA replicative polymerases. *Nucleic Acids Res. 40*, 6174−6186.
(65) Long, X., Parks, J. W., Bagshaw, C. R., and Stone, M. D. (2013) Mechanical unfolding of human telomere G-quadruplex DNA probed by integrated fluorescence and magnetic tweezers spectroscopy. *Nucleic Acids Res. 41*, 2746−2755.
(66) Wuite, G. J. L., Smith, S. B., Young, M., Keller, D., and Bustamante, C. (2000) Single-molecule studies of the effect of template tension on T7 DNA polymerase activity. *Nature 404*, 103−106.
(67) Lormand, J. D., Buncher, N., Murphy, C. T., Kaur, P., Lee, M. Y., Burgers, P., Wang, H., Kunkel, T. A., and Opresko, P. L. (2013) DNA polymerase *δ* stalls on telomeric lagging strand templates independently from G-quadruplex formation. *Nucleic Acids Res. 41*, 10323−10333.
(68) Hogg, M., Osterman, P., Bylund, G. O., Ganai, R. A., Lundstrom, E. B., Sauer-Eriksson, A. E., and Johansson, E. (2013) Structural basis for processive DNA synthesis by yeast DNA polymerase *ε*. *Nat. Struct. Mol. Biol. 21*, 49−55.
(69) Brautigam, C. A., and Steitz, T. A. (1998) Structural and functional insights provided by crystal structures of DNA polymerases and their substrate complexes. *Curr. Opin. Struct. Biol. 8*, 54−63.
(70) Swan, M. K., Johnson, R. E., Prakash, L., Prakash, S., and Aggarwal, A. K. (2009) Structural basis of high-fidelity DNA synthesis by yeast DNA polymerase *δ*. *Nat. Struct. Mol. Biol. 16*, 979−986.
(71) Aksenova, A., Volkov, K., Maceluch, J., Pursell, Z. F., Rogozin, I. B., Kunkel, T. A., Pavlov, Y. I., and Johansson, E. (2011) Mismatch repair-independent increase in spontaneous mutagenesis in yeast lacking non-essential subunits of DNA polymerase epsilon. *PLoS Genet. 6*, e1001209.
(72) Choi, J., Park, J., Tanaka, A., Park, M. J., Jang, Y. J., Fujitsuka, M., Kim, S. K., and Majima, T. (2012) Hole trapping of G-quartets in a G-quadruplex. *Angew. Chem., Int. Ed. 52*, 1134−1138.
(73) Vorlickova, M., Tomasko, M., Sagi, A. J., Bednarova, K., and Sagi, J. (2011) 8-Oxoguanine in a quadruplex of the human telomere DNA sequence. *FEBS J. 279*, 29−39.

DOI: 10.1021/acs.biochem.5b00060
Biochemistry 2015, 54, 3218−3230